2023 IEEE 26th International Conference on
Intelligent Transportation Systems (ITSC)
24-28 September 2023. Bilbao, Bizkaia, Spain

Adaptive Signalized Intersection Control in Mixed Traffic Environment of Connected Vehicles with Safety Guarantees

Sanghoon Oh[1], Qi Chen[2], H. Eric Tseng[2], Gaurav Pandey[2], and Gábor Orosz[1,3]

***Abstract*— Adaptive signalized intersection control with safety guarantees is proposed for a connected intersection serving mixed traffic consisting of automated and human-driven vehicles. To assure safety, we utilize backward reachable tubes to ensure that the conflict zone is not reached simultaneously by two vehicles. The backward reachable tubes of given initial conditions can be computed offline and stored on the cloud (or infrastructure). The high-level decision determines the signals along with a proposed trajectory for the connected automated vehicle, in order to strive for traffic efficiency while ensuring safety. We start with two vehicles (one connected automated vehicle and one connected human vehicle) and demonstrate traffic efficiency and safety assurance with numerical simulations under a wide range of scenarios. We show that, with respect to the worst trip delay, the proposed strategy outperforms the benchmark of a heuristic traffic management algorithm.**

I. INTRODUCTION

Vehicle-to-everything (V2X) communication has the potential to enhance automation in various ways, such as overcoming line-of-sight restrictions and boosting safety and efficiency [1]. Intersection control is a good example of the utilization of connectivity to improve throughput and safety at the same time.

One may categorize existing studies on intersection control based on their approaches. Many works assume a 100 percent penetration rate of connected automated vehicles (CAVs) and then apply optimization-based methods [2], [3], [4], [5]. Under such an assumption, the problem transforms into a mixed-integer nonlinear optimization problem, wherein discrete decision variables represent which lane holds priority in passing the intersection. A cooperative dynamic intersection protocol for CAVs called cyber traffic signal was shown to have superior performance in terms of worst trip delay compared to the traditional stop-and-yield policy [6]. On the other hand, reservation-based methods reserve temporal and spatial slots based on incoming requests and use predefined sorting methods for scheduling [7]. For example, in [8], a legacy algorithm that can efficiently control the intersection with low penetration of connected vehicles was suggested, while safety and efficiency improvements via a priority-based method in SUMO simulation environment was demonstrated [9].

[1]Sanghoon Oh and Gábor Orosz are with the Department of Mechanical Engineering, University of Michigan, Ann Arbor, MI 48109, USA {osh,orosz}@umich.edu

[2]Qi Chen, Eric Tseng and Gaurav Pandey are with Ford Motor Company, Dearborn, MI 48124, USA {qchen51,htseng,gpandey2}@ford.com

[3]Gábor Orosz is also with the Department of Civil and Environmental Engineering, University of Michigan, Ann Arbor, MI 48109, USA

Due to the challenging nature of attaining a complete adoption of automated vehicles in the near future, some researchers considered connected intersection control/planning methods under reduced penetration rates of CAVs [10], [11]. Taking into account the uncertainty of human-driven vehicles in mixed traffic, a polynomial-time approximation scheme for intersection control with CAVs was suggested [12], and mixed integer programming was used to construct a decentralized, hybrid network control policy that maximizes throughput [13]. However, mixed integer programming is known to be computationally very expensive, which can motivate the use of heuristics like first-come-first-serve (FCFS) methods. For example, the alternating direction method of multipliers (ADMM) is used to decompose the roundabout optimal trajectory planning problem into solvable small ones [14]. Also, an FCFS-type reservation-based intersection control method called hybrid autonomous intersection management was proposed for mixed traffic scenarios [15].

There has been some interest in methods that can rigorously keep safety considering the dynamics of vehicles. Hamilton-Jacobi (HJ) reachability is a strong analytical tool that can provide the control invariant safe region in the state space by computing forward or backward reachable states using differential games [16], [17], [18], [19]. HJ reachability provides flexibility for setting different formulations of dynamics, target sets, and disturbances [20]. However, one must take utmost care when setting up the problem since the main challenge of HJ reachability is that its computational complexity grows exponentially with the state space dimension. The level set toolbox provides an efficient implementation of HJ reachability computation in MATLAB environment [21].

In this paper, we propose an HJ reachability-based method that enables safe control of a connected signalized intersection with mixed traffic to bridge the gap between microscopic dynamical safety and macroscopic traffic efficiency. First, a brief overview of HJ reachability-based safety verification is given in a general problem setting, which is based on the computation of the backward reachability tube (BRT). Then, the vehicle dynamics, the goal sets, and the conflict set are defined for a mixed traffic scenario when a connected automated vehicle (CAV) and a connected human-driven vehicle (CHV) appear in a two-way intersection. A higher-level decision for intersection control is introduced utilizing the BRTs of different goal sets and corresponding lower-level plans are also derived using the least-restrictive approach. Numerical simulations are used to demonstrate the safety of the designed algorithms. The worst trip delay is evaluated

and compared to that of a benchmark algorithm to show the potential benefit in terms of time efficiency when our algorithm used in macroscopic traffic management.

II. Hamilton-Jacobi Reachability

In this section, a brief overview of HJ reachability is given. Let us define the state $x \in \mathbb{R}^n$, the input $u \in \mathcal{U}$, and the disturbance $d \in \mathcal{D}$, where the latter accounts for a bounded uncertain portion of the input. Here, $\mathcal{U} \subset \mathbb{R}^m$ denotes a compact set of admissible inputs and $\mathcal{D} \subset \mathbb{R}^l$ denotes a compact set of bounded disturbances. Then the dynamics can be formulated as

$$\dot{x}(t) = f\big(x(t), u(t), d(t)\big). \tag{1}$$

If the function $f : \mathbb{R}^n \times \mathcal{U} \times \mathcal{D} \to \mathbb{R}^n$ is uniformly continuous, bounded, and Lipschitz continuous then for given initial condition x_0 (taken at time 0), input profile $u(\cdot)$ and disturbance profile $d(\cdot)$, the solution ζ is unique and can be defined as

$$\begin{aligned} &\frac{\mathrm{d}}{\mathrm{d}t}\zeta(t; x_0, u(\cdot), d(\cdot)) = f\big(\zeta(t; x_0, u(\cdot), d(\cdot)), u(t), d(t)\big), \\ &\zeta(0; x_0, u(\cdot), d(\cdot)) = x_0. \end{aligned} \tag{2}$$

The backward reachable tube (BRT) represents the set of states $x_0 \in \mathbb{R}^n$ from which the state can get into the goal set $\mathcal{G} \subset \mathbb{R}^n$ while avoiding the conflict set $\mathcal{C} \subset \mathbb{R}^n$ in time $T \geq 0$. Mathematically this can be formulated as

$$\begin{aligned} \text{BRT}(T, \mathcal{G}, \mathcal{C}) = \{x_0 : \forall d \in \mathcal{D}, \exists u \in \mathcal{U}, \\ \exists t, 0 \leq t \leq T, \zeta(t; x_0, u(\cdot), d(\cdot)) \in \mathcal{G}, \\ \forall t, 0 \leq t \leq T, \zeta(t; x_0, u(\cdot), d(\cdot)) \notin \mathcal{C}\}. \end{aligned} \tag{3}$$

The BRT analysis can be turned into a HJ reachability problem by computing a value function (defined below in (6)) whose sub-zero level set gives the BRT. The goal set $\mathcal{G}$ is expressed as a sub-zero level set of the function $l : \mathbb{R}^n \to \mathbb{R}$:

$$\mathcal{G} = \{x : l(x) \leq 0\}, \tag{4}$$

while the conflict set $\mathcal{C}$ is expressed as a super-zero level set of the function $k : \mathbb{R}^n \to \mathbb{R}$:

$$\mathcal{C} = \{x : k(x) \geq 0\}. \tag{5}$$

In order to formulate the optimization problem, we define a value function as

$$V(x, T) = \min_u \max_d \min_{t \in [0,T]} \max\big\{l(x(t)), \max_{\sigma \in [0,t]}\{k(x(\sigma))\}\big\}. \tag{6}$$

It can be shown [22] that the value function (6) is the same as the viscosity solution of the Hamilton-Jacobi-Isaacs (HJI) partial differential equation

$$\begin{aligned} &\max\big\{\partial_t V(x,t) + \min\{0, H(x, \lambda, t)\}, k(x) - V(x,t)\big\} = 0, \\ &V(x(T), T) = l(x(T)). \end{aligned} \tag{7}$$

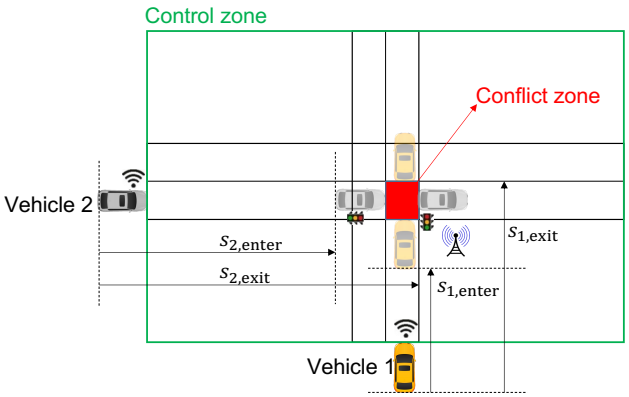

Fig. 1. Definitions of control and conflict zones

Here the Hamiltonian $H(x, \lambda, t)$ is defined as

$$\begin{aligned} H(x, \lambda, t)) = \min_u \max_d \lambda \cdot f(x, u, d), \\ \lambda = \partial_x V(x, t), \end{aligned} \tag{8}$$

and $\cdot$ denotes the dot product of vectors in $\mathbb{R}^n$. We remark that a more general Hamiltonian may be defined [20], [23], but the form defined here is adequate for the intersection problem analyzed below. The value function can be obtained numerically using the level set toolbox [21].

III. Connected Intersection Control

A. Intersection Layout

The intersection layout is illustrated in Fig. 1 for a general four-way intersection setting. The control zone is the area where the vehicles are affected by the traffic signal (whose phase may also be communicated to them via V2X). The conflict zone is the area where a collision can happen when two agents (arriving from different directions) are present at the same time. All vehicles are assumed to keep their lane and only their longitudinal motions are modeled. In the illustrated scenario, one vehicle is passing the intersection from the west and the other is entering from the south. We remark that our setup may be generalized to a large set of conflicting intersection maneuvers (including turning). In this paper, we limit our attention to a two-vehicle conflict resolution setting, where the vehicles are passing the intersection from different directions.

Traveled distances s_1 and s_2 of the vehicles are measured based on their rear ends such that $s_i = 0, i = 1, 2$ when entering the control zone. Moreover, $s_{i,\text{enter}}, i = 1, 2$ denote the traveled distances when the front bumpers of the vehicles enter the conflict zone, while $s_{i,\text{exit}}, i = 1, 2$ denote the traveled distances once the rear bumpers of the vehicles exit the conflict zone. For simplicity, the total lengths of vehicles are assumed to be the same and known. The actual size of the zone used for simulation is defined in Section V.

B. Dynamics and Constraints

In the two-vehicle conflict resolution problem defined above, double-integrator dynamics are used to express the longitudinal motion of both vehicles. It is assumed vehicle 1

is a connected automated vehicle (CAV) while vehicle 2 is a connected human-driven vehicle (CHV). Thus, variables with subscript 1 refer to the states of the CAV while variables with subscript 2 refer to the statesof the CHV. We define the 4-dimensional state $x \in \mathbb{R}^4$ by including traveled distances $s_i, i = 1, 2$ and longitudinal velocities $v_i, i = 1, 2$, that is,

$$x = [s_1, v_1, s_2, v_2]^\top. \tag{9}$$

Then the dynamics are expressed as

$$\dot{x} = \begin{bmatrix} 0 & 1 & 0 & 0 \\ 0 & 0 & 0 & 0 \\ 0 & 0 & 0 & 1 \\ 0 & 0 & 0 & 0 \end{bmatrix} x + \begin{bmatrix} 0 \\ 1 \\ 0 \\ 0 \end{bmatrix} u + \begin{bmatrix} 0 \\ 0 \\ 0 \\ 1 \end{bmatrix} d. \tag{10}$$

The state constraint is specified as

$$0 \le v_1 \le v_{\text{max}}, \qquad 0 \le v_2 \le v_{\text{max}}, \tag{11}$$

and the acceleration of vehicle 1 is defined as the input of the system which is bounded as

$$u_{\text{min}} \le u \le u_{\text{max}}. \tag{12}$$

The unknown input of vehicle 2 is defined as a disturbance of the dynamics and this is assumed to be bounded as

$$d_{\text{min}} \le d \le d_{\text{max}}. \tag{13}$$

C. Conflict and Goal Sets

Based on the intersection layout defined above, we define the conflict set $\mathcal{C}$ in the 4-dimensional state space as

$$\begin{aligned} \mathcal{C} = \{x = [s_1, v_1, s_2, v_2]^\top : \\ s_{1,\text{enter}} \le s_1 \le s_{1,\text{exit}}, s_{2,\text{enter}} \le s_2 \le s_{2,\text{exit}}\}. \end{aligned} \tag{14}$$

The conflict set indeed corresponds to those states where vehicles 1 and 2 occupy the conflict zone at the same time.

The objective of the intersection control is to find a decision that has a time-efficient future motion for the CAV such that the trajectory does not pass the conflict set while reaching the goal set. Here we define two different goal sets, which both are closed sets in state space, based on two different higher-level plans. The first goal corresponds to the CAV (vehicle 1) clearing the conflict zone first before the CHV (vehicle 2) enters. The corresponding set in state space is defined as

$$\begin{aligned} \mathcal{G}_1 = \{x = [s_1, v_1, s_2, v_2]^\top : \\ s_{1,\text{exit}} \le s_1 \le s_{\text{large}}, 0 \le s_2 \le s_{2,\text{enter}}, \\ 0 \le v_1 \le v_{\text{max}}, 0 \le v_2 \le v_{\text{max}}\}, \end{aligned} \tag{15}$$

which is illustrated in Fig. 2. Here s_{large} is a large positive real value. Similarly, the second goal corresponds to the CHV (vehicle 2) passing first while the CAV (vehicle 1) gives the way with the corresponding goals set being

$$\begin{aligned} \mathcal{G}_2 = \{x = [s_1, v_1, s_2, v_2]^\top : \\ s_{2,\text{exit}} \le s_2 \le s_{\text{large}}, 0 \le s_1 \le s_{1,\text{enter}}, \\ 0 \le v_1 \le v_{\text{max}}, 0 \le v_2 \le v_{\text{max}}\}. \end{aligned} \tag{16}$$

By computing value functions V_1 and V_2 corresponding to different goals $\mathcal{G}_1$ and $\mathcal{G}_2$, we can determine the reachability of the lower-level plans based on different high-level plans.

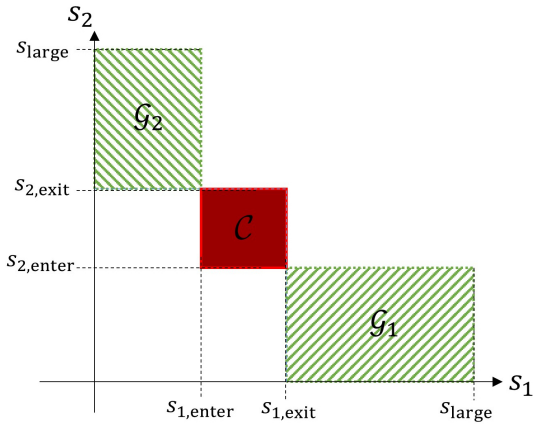

Fig. 2. Definitions of goal and conflict sets

IV. Reachability-Based Intersection Control

A safety condition for the state constraints (11), input constraints (12), and disturbance bounds (13) is computed based on the value function obtained as the solution of the HJI partial differential equation (7). Using the level set toolbox we compute the value functions $V_i, i = 1, 2$ in every grid point in the (discretized) state space. The subzero level set of the value function V_i represents the backward reachable tube of the goal set $\mathcal{G}_i$ and time T. One may also calculate the minimum time required for the given state to reach a goal set safely, that is, define the time window

$$T_{\text{w},i}(x) = \min_T \left\{x \in \text{BRT}(T, \mathcal{G}_i, \mathcal{C})\right\}. \tag{17}$$

Based on the computation of value functions for different T values and different goal sets, we can determine if the given state is backward reachable in finite time or not. If the value function at a state is smaller than zero for any finite time T, we consider the state to be backward reachable. If the given state is in the backward reachable tube of the corresponding goal with a finite time-to-reach value, then there exist a safe input trajectory which can lead the state to the goal set in finite time without entering the conflict set. The backward reachability of a given initial condition implies the safety of the decision, which we can translate to a sufficient safety condition. Based on this safety condition and the time window (17), we can define three different higher-level plans as laid out in Algorithm 1. Note that, however, in the current problem setting, backward reachability is not the necessary and sufficient condition of safety. That is, there exist states which are not backward reachable from a goal set, while a safe trajectory to that goal set can still be found.

Algorithm 1 is triggered once both vehicles enter the control zone defined in Fig. 1. Since vehicles do not necessarily enter the zone at the same time, the algorithm will be triggered at the moment when the later vehicle enters the zone. Once the higher-level plan is determined, it is not changed until the goal is reached as we do not want to change the traffic signal for the human-driven vehicle once it is already inside the control zone.

Algorithm 1 High-level decision plan

if $T_{\mathrm{w},1}(x) < \infty$ & $T_{\mathrm{w},1}(x) \leq T_{\mathrm{w},2}(x)$ **then**
decision 1: Assign green light to CHV, let CAV pass first
else if $T_{\mathrm{w},2}(x) < \infty$ & $T_{\mathrm{w},2}(x) < T_{\mathrm{w},1}(x)$ **then**
decision 2: Assign green light to CHV, let CAV pass second
else
decision 3: Assign red light to CHV, let CAV pass first
end if

The safety controller is given by the optimal input as a function of the state. That is, for goal i we have

$$u_i^*(x) = \underset{u}{\operatorname{argmin}} \max_{d} \{\partial_t V_i \cdot f(x,u,d)\}, \tag{18}$$

that drives the value function to its minimum under the worst-case disturbance. Since the input of CHV is treated as a disturbance of the system, it can only be indirectly controlled by the intersection server, i.e., by using the traffic light. However, the worst-case behavior of CHV that threatens safety is considered to be the optimal disturbance for the system, which for goal i can be formulated as

$$d_i^*(x) = \underset{d}{\operatorname{argmax}} \min_{u} \{\partial_x V_i \cdot f(x,u,d)\}. \tag{19}$$

Based on the dynamics (10), the intersection server is assumed to have the planning authority over the longitudinal motion of the CAV. To achieve both time efficiency and safety of the motion, the least restrictive control

$$u_i(x) = \begin{cases} u_{\mathrm{d}} & \text{if} \quad V_i(x) < \mathrm{th}, \\ u_i^*(x) & \text{if} \quad V_i(x) \geq \mathrm{th}, \end{cases} \tag{20}$$

is applied when generating the low-level plan. That is, the safety controller (optimal input) is only applied when the value of the state is close to 0 (greater than a small negative value th). Note that the threshold th is selected based on the discretization of the state space and this also serves as a safety margin. If the value is far from 0, the desired control denoted by u_{d} is applied which leads to time efficiency. In this problem, the desired control has the explicit form $u_{\mathrm{d}} = u_{\max}$ if $v_1 < v_{\max}$ and $u_{\mathrm{d}} = 0$ if $v_1 = v_{\max}$, but it can also be implicitly computed online if a cost function that the desired control should minimize is defined. In order to generate the low-level plan of the trajectory, the least-restrictive control (20) and optimal disturbance (19) is applied to (10) with given initial condition and integrated up to the point where the corresponding goal is reached.

V. Numerical Results

We conducted numerical simulations for a wide range of initial conditions with the following parameters defining the boundaries of control and conflict zones (cf. Fig. 1), the limits on actuation authorities of CAV, and the range of disturbances caused by the CHV: $s_{1,\mathrm{enter}} = s_{2,\mathrm{enter}} = 20\,\mathrm{m}$, $s_{1,\mathrm{exit}} = s_{2,\mathrm{exit}} = 25\,\mathrm{m}$, $v_{\max} = 20\,\mathrm{m/s}$, $u_{\min} = -8\,\mathrm{m/s^2}$, $u_{\max} = 3\,\mathrm{m/s^2}$, $-d_{\min} = d_{\max} = 1\,\mathrm{m/s^2}$, $\mathrm{th} = -0.2$.

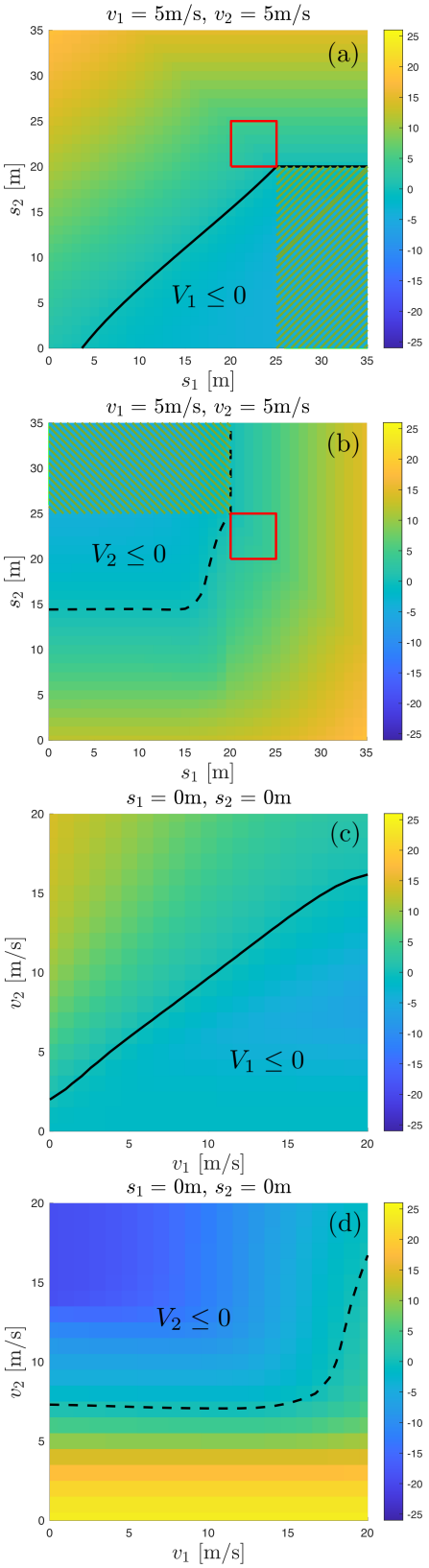

Fig. 3. Value function in case of $T = 3$ seconds time to reach goal 1 (panels (a,c)) and goal 2 (panels (b,d)). For panels (a,b) the values of v_1 and v_2 are fixed as indicated. For panels (c,d), the values of s_1 and s_2 are fixed as indicated. The values are shown using color maps. Solid black curves highlight the boundaries of the BRT for goal 1 and dashed black curves show the boundaries of the BRT for goal 2.

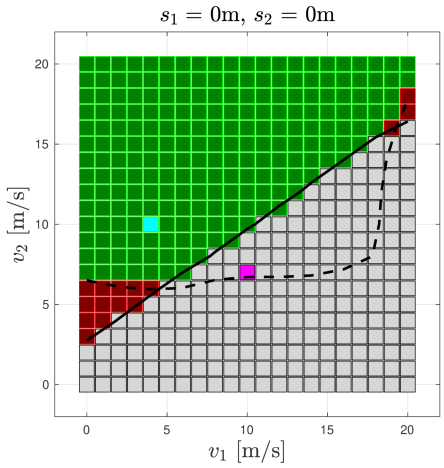

Fig. 4. High-level decision plan. Gray squares indicate states with decision 1 (green light to CHV and pass CAV first), green ones are for decision 2 (green light to CHV and pass CAV second), while the red ones are for decision 3 (red light to CHV and pass CAV first). Magenta and cyan blocks mark the initial conditions used for the low-level plans in Figs. 5 and 6, respectively. The solid black curve represents the boundary of the BRT for goal 1, and the dashed black curve represents the boundary of the BRT for goal 2.

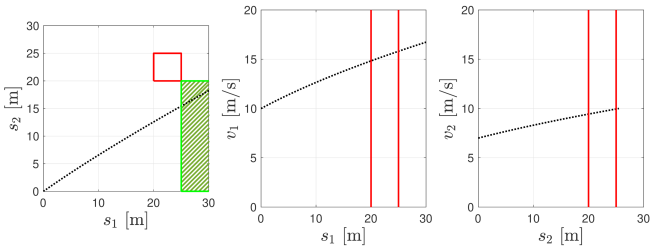

Fig. 5. Low-level plan under worst-case disturbance for decision 1 (green light to CHV and pass CAV first)

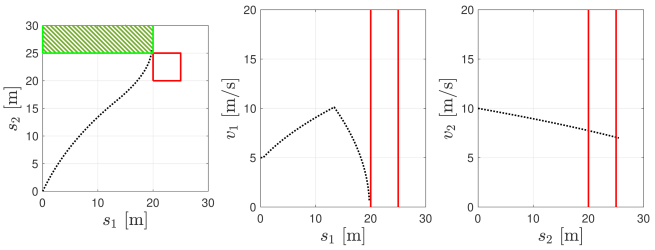

Fig. 6. Low-level plan under worst-case disturbance for decision 2 (green light to CHV and pass CAV second)

A. *Value function and high-level decision chart*

The obtained value functions are illustrated in the (s_1, s_1)-plane in Fig. 3(a) and (b) for the goal sets $\mathcal{G}_1$ and $\mathcal{G}_2$, respectively. Here the velocities are set to $v_1 = v_2 = 5\,\mathrm{m/s}$ and the time to reach is $T = 3\,\mathrm{s}$. The red rectangle bounds of the conflict set $\mathcal{C}$, while the green shaded domains show the sets $\mathcal{G}_1$ and $\mathcal{G}_2$. Values for different states are depicted using color maps, and the zero boundaries of the values, i.e., boundaries of BRTs, are highlighted as solid black and dashed black curves. For the same time window, since the system is assumed to have no direct control authority over the CHV, the BRT of $\mathcal{G}_2$ is smaller than the BRT of $\mathcal{G}_1$, which means letting CAV pass the conflict zone first safely has larger set assigned to in the state space. Value functions for goal sets $\mathcal{G}_1$ and $\mathcal{G}_2$ are also illustrated in the (v_1, v_1)-plane in Fig. 3(c) and (d), respectively, for positions $s_1 = s_2 = 0\,\mathrm{m}$ and time to reach $T = 3\,\mathrm{s}$. Based on the system dynamics (10) and the gradient of the value functions one may calculate the optimal (best case) input (18) and the optimal (worst case) disturbance (19).

Fig. 4 shows the high-level decision chart in the (v_1, v_1)-plane for $s_1 = s_2 = 0\,\mathrm{m}$. Since both vehicles are placed at the same distance from the conflict zone, states with higher v_1 lead to a plan that lets vehicle 1 (CAV) pass first while states with higher v_2 lead to a plan that lets vehicle 2 (CHV) pass first (except for the cases where vehicle 1 has very low speed and vehicle 2 is a little bit faster). However, since the intersection only has authority over vehicle 1 only, the region for decision 1 (green light to CHV and pass CAV first) is larger than the region of decision 2 (green light to CHV and pass CAV second).

B. *Low-level plan and trip delay*

Fig. 5 shows the trajectory of the low-level plan for decision 1 when using (20) in (10) while the CHV exhibits the worst-case behavior in terms of safety based on (19). One may observe that the CAV tries to clear the conflict zone as fast as possible while the CHV tries to create the conflict by accelerating to the maximum. Similarly, Fig. 6 illustrates the trajectory of CHV and CAV under decision 2, showcasing the worst-case behavior of CHV. In this scenario, CAV's low-level control aims to pass the intersection expeditiously but ensures it follows CHV to prevent any conflicts. It can be observed that CAV accelerates initially (to minimize trip delay) until it reaches the point where it must decelerate to avoid entering the conflict zone before CHV exits.

To evaluate the potential benefit of the proposed planning algorithm for traffic management, we compare the result to the heuristic FCFS algorithm given in [15] that serves as the benchmark. Here, we measure the worst trip delay, which is the larger trip delay of two vehicles. In the proposed two vehicle example, the worst trip delay is equal to total delay, which is more popular metric for traffic efficiency and can be considered in the scaled-up version of the algorithm. Fig. 7 shows the worst trip delay evaluation result compared to the FCFS algorithm. For the initial condition considered, both the FCFS algorithm and our proposed algorithm let vehicle 2 (CHV) pass first. Fig. 8 shows the evaluated worst trip delays for initial conditions where FCFS algorithm lets vehicle 2 (CHV) pass first while our proposed algorithm lets vehicle 1 (CAV) pass first. In both cases, the proposed algorithm significantly outperforms FCFS in terms of the worst trip delay.

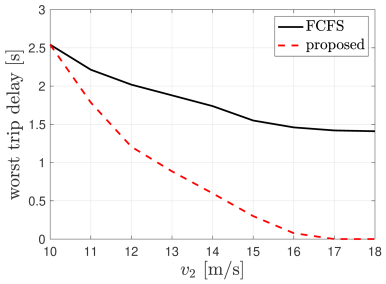

Fig. 7. Worst trip delay comparison between the FCFS and the proposed algorithms when the high-level decisions are the same for both algorithms for various initial conditions in v_2. The initial conditions of other state variables are $(s_1, v_1, s_2) = (0\,\text{m}, 10\,\text{m/s}, 2\,\text{m})$.

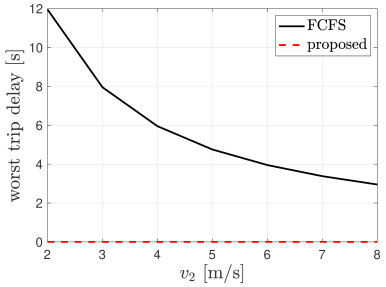

Fig. 8. Worst trip delay comparison between the FCFS and the proposed algorithms when high-level decisions are different for the two algorithms for various initial conditions of v_2. Initial conditions of other state variables to $(s_1, v_1, s_2) = (0\,\text{m}, 10\,\text{m/s}, 2\,\text{m})$.

VI. Conclusion

Adaptive control of a signalized intersection with connected mixed traffic that can guarantee safety was proposed. Assuming the known capabilities of a CAV and a CHV and treating CHV's input as disturbance with known bounds, one can compute backward reachability tubes offline and use the corresponding safety conditions to make real-time high-level signal decisions. While safety is a priority, the time efficiency of the lower-level motion plan is also taken into account, and the least restrictive plan for generating CAV's motion is applied to achieve the lowest trip delay. This approach outperforms a benchmark traffic management algorithm applied to the same problem in terms of trip delay. Future work includes adding the consideration of potential delays in the actuation of CAV and in V2X communication. Driver models with uncertainties will also be introduced to better represent CHV behaviors. The algorithm will also be scaled up for a large number of vehicles by integrating the pairwise conflict resolution problem into macroscopic intelligent traffic management systems without adding additional dimensions to the reachability computation.

References

[1] T. Ersal, I. Kolmanovsky, N. Masoud, N. Ozay, J. Scruggs, R. Vasudevan, and G. Orosz, "Connected and automated road vehicles: state of the art and future challenges," *Vehicle System Dynamics*, vol. 58, no. 5, pp. 672–704, 2020.

[2] M. Al-Turki, N. T. Ratrout, S. M. Rahman, and K. J. Assi, "Signalized intersection control in mixed autonomous and regular vehicles traffic environment – A critical review focusing on future control," *IEEE Access*, vol. 10, pp. 16 942–16 951, 2022.

[3] L. Chen and C. Englund, "Cooperative intersection management: A survey," *IEEE Transactions on Intelligent Transportation Systems*, vol. 17, no. 2, pp. 570–586, 2015.

[4] J. Lee and B. Park, "Development and evaluation of a cooperative vehicle intersection control algorithm under the connected vehicles environment," *IEEE Transactions on Intelligent Transportation Systems*, vol. 13, no. 1, pp. 81–90, 2012.

[5] M. W. Levin and D. Rey, "Conflict-point formulation of intersection control for autonomous vehicles," *Transportation Research Part C*, vol. 85, pp. 528–547, 2017.

[6] S. Aoki and R. Rajkumar, "Cyber traffic light: Safe cooperation for autonomous vehicles at dynamic intersections," *IEEE Transactions on Intelligent Transportation Systems*, vol. 23, no. 11, pp. 22 519–22 534, 2022.

[7] K. Dresner and P. Stone, "Multiagent traffic management: A reservation-based intersection control mechanism," in *Joint Conference on Autonomous Agents and Multiagent Systems, International*, vol. 3, 2004, pp. 530–537.

[8] L. C. Bento, R. Parafita, S. Santos, and U. Nunes, "Intelligent traffic management at intersections: Legacy mode for vehicles not equipped with V2V and V2I communications," in *16th IEEE International Conference on Intelligent Transportation Systems (ITSC)*, 2013, pp. 726–731.

[9] X. Qian, J. Gregoire, F. Moutarde, and A. De La Fortelle, "Priority-based coordination of autonomous and legacy vehicles at intersection," in *17th IEEE Intelligent Transportation Systems Conference (ITSC)*, 2014, pp. 1166–1171.

[10] Z. Yao, B. Zhao, T. Yuan, H. Jiang, and Y. Jiang, "Reducing gasoline consumption in mixed connected automated vehicles environment: A joint optimization framework for traffic signals and vehicle trajectory," *Journal of Cleaner Production*, vol. 265, p. 121836, 2020.

[11] S. Aoki and R. Rajkumar, "V2V-based synchronous intersection protocols for mixed traffic of human-driven and self-driving vehicles," in *25th International Conference on Embedded and Real-Time Computing Systems and Applications (RTCSA)*, 2019, pp. 1–11.

[12] M. Abdolmaleki, Y. Yin, and N. Masoud, "A unifying graph-coloring approach for intersection control in a connected and automated vehicle environment," *Available at SSRN 3944348*, 2021.

[13] D. Rey and M. W. Levin, "Blue phase: Optimal network traffic control for legacy and autonomous vehicles," *Transportation Research Part B*, vol. 130, pp. 105–129, 2019.

[14] R. Mohebifard and A. Hajbabaie, "Trajectory control in roundabouts with a mixed fleet of automated and human-driven vehicles," *Computer-Aided Civil and Infrastructure Engineering*, vol. 37, no. 15, pp. 1959–1977, 2022.

[15] G. Sharon and P. Stone, "A protocol for mixed autonomous and human-operated vehicles at intersections," in *International Conference on Autonomous Agents and Multiagent Systems*, 2017, pp. 151–167.

[16] I. M. Mitchell, A. M. Bayen, and C. J. Tomlin, "A time-dependent Hamilton-Jacobi formulation of reachable sets for continuous dynamic games," *IEEE Transactions on Automatic Control*, vol. 50, no. 7, pp. 947–957, 2005.

[17] M. Althoff and J. M. Dolan, "Online verification of automated road vehicles using reachability analysis," *IEEE Transactions on Robotics*, vol. 30, no. 4, pp. 903–918, 2014.

[18] M. Chen, J. C. Shih, and C. J. Tomlin, "Multi-vehicle collision avoidance via Hamilton-Jacobi reachability and mixed integer programming," in *55th Conference on Decision and Control (CDC)*, 2016, pp. 1695–1700.

[19] A. Bajcsy, S. L. Herbert, D. Fridovich-Keil, J. F. Fisac, S. Deglurkar, A. D. Dragan, and C. J. Tomlin, "A scalable framework for real-time multi-robot, multi-human collision avoidance," in *International Conference on Robotics and Automation (ICRA)*, 2019, pp. 936–943.

[20] S. Bansal, M. Chen, S. Herbert, and C. J. Tomlin, "Hamilton-Jacobi reachability: A brief overview and recent advances," in *56th Conference on Decision and Control (CDC)*, 2017, pp. 2242–2253.

[21] I. M. Mitchell, "A toolbox of level set methods," University of British Columbia, Department of Computer Science, Tech. Rep. TR-2007-11, 2007.

[22] L. C. Evans and P. E. Souganidis, "Differential games and representation formulas for solutions of Hamilton-Jacobi-Isaacs equations," *Indiana University Mathematics Journal*, vol. 33, no. 5, pp. 773–797, 1984.

[23] Z. Li, "Comparison between safety methods control barrier function vs. reachability," *arXiv: 2106.13176*, 2021.